Zhongguo Kuangye Daxue Xuebao
Journal of China University of Mining and Technology

2024 | Vol 29 | Issue 3 | Page 230-241
Journal Homepage: https://zkdx.ch/
DOI: 10.1654/zkdx.2024.29.3-19

Influence of Using Composite Materials on the Behavior of Reinforced Concrete Columns

Mohamed M. Badawy
Civil Engineering Department, High Institute for Engineering and Technology at Al-Obour, Cairo, Egypt

Mahmoud Y. A. Zaghlal
Civil Engineering Department, Faculty of Engineering, Zagazig University, Zagazig, Vice dean, High Institute for Engineering and Technology at Al-Obour, Cairo, Egypt

Khaled Fawzy
Civil Engineering Department, Faculty of Engineering, Zagazig University, Zagazig, Vice dean, High Institute for Engineering and Technology at Al-Obour, Cairo, Egypt

Azza I. Anan*
Civil Engineering Department, High Institute for Engineering and Technology at Al-Obour, Cairo, Egypt
*Corresponding author

Abstract
A large capacity of columns to withstand highly loads without negatively affecting the architectural requirements is one of the most important challenges facing the construction concept. One of the recent methods of strengthening columns is the use of glass or carbon fiber reinforced polymers (GFRP) or (CFRP) laminates. Five experimental prototype columns with dimensions 200x200x1200 mm for width, length and height were examined under axial compression load. The first column specimen without any is strengthening wrapping to be considered a control specimen. The other four column specimens strengthened by CFRP and GFRP wrapping using fully and partially confinement techniques. The experimental results showing a good enhancement in loading capacity by 16% and 40% for partially and fully CFRP wrapping respectively. Consequently, a slight improvement by 11% and 19% in loading capacity for column specimens with partially and fully GFRP wrapping respectively. Also, the mechanism of failure and for strengthened columns by CFRP or GFRP transferred to FRP rupture instead of concrete crushing. This confirmed that the fiber sheets were fully bonded to concrete from the loading beginning up to failure. Finite element (FE) program was conducted using ANSYS software to recognize deeply the behavior of laminates made of GFRP and CFRP.

Keywords
Strengthening, Wrapping, Confinement, Laminates, Bonding, Columns

1. Introduction
Concrete constructions frequently demand strengthening to enhance their load-bearing capacity. This strengthening may have been needed due to a modification in utilize that resulted in extra living loads, such as an evolution in the use of the property from housing to publicly traded or storage spaces. design errors, building process challenges during construction, or building rehabilitations to meet current safety codes. Columns are commonly strengthened using concrete jacketing, steel jacketing and fiber reinforced polymer (FRP) jacketing. All of these strategies have been found to significantly enhance the axial loading ability of columns.

1.1 Previous Research Work
Usage of confined carbon and glass fibers laminates are considered innovative ways to improve loading capacity of columns [1-2]. For purposes of construction, square or rectangle columns are preferred and popular because they are easier to build than circular columns.

Reinforced concrete constructions frequently need strengthening to improve their load bearing capacity [3].

An experimental and theoretical study of twenty square reinforced concrete columns reinforced with steel jackets [4]. It was discovered that the compressive strength of enhanced square reinforced concrete columns with a complete steel jacket was more than double that of control columns without strengthening.

Externally wrapped fiber-reinforced polymers (FRP) have revolutionized the construction industry with their remarkable properties, including resistance to corrosion and a high strength-to-weight ratio [5-6].

Wrapping parameters such as full wrapping, partially wrapping are used. An earlier study described an equivalent wrapping approach [7]. A mathematical approach for predicting the moment curving response of reinforced concrete columns limited by angles and battens, as well as validation by investigation using thirteen specimens subjected to axial forces.

It was shown that the theoretical model also accurately anticipated the flexural and resistance actions of columns reinforced with angles and battens. [8].

An integrated stress-strain model with varied cross-sectional concrete columns confined by FRP were provided [9-16]. Concrete cross sections that were square, rectangular, and circular were used. A straightforward and precise model of the equivalent corner radius ratio for circular, square, and rectangular columns was provided based on the data currently available about the behavior of these column shapes enclosed by FRP jackets.

A modeling and monotonic axial behavior of RC circular columns required by CFRP was created. [17]. Twenty-five reinforced concrete columns that were constrained by CFRP composites were part of the experimental program. The diameter of the columns, the kind of material (plain or reinforced concrete), the distance between the steel hoop of the RC columns, and the quantity of CFRP layers were the variables of the columns. Based on the experimental study, predictive equations were developed to determine the axial or lateral failure strain of circular reinforced concrete columns jacketed with CFRP, the maximum axial load, and the compressive strength of the confined concrete. According to the study's conclusions, the two types of CFRP that were used demonstrated good performance, and the compressive strength of the concrete columns increased as the number of CFRP plies increased. The models with smaller diameters had significantly higher compression strengths than the larger ones.

Thus far, it appears that insufficient research has been done on how utilizing wrapped fiber reinforced polymers affects the strength of short concrete columns. Thus, the purpose of this study is to examine how short columns reinforced with advanced composite materials behave generally whether wrapped completely or partially. Consequently, whether CFRP or GFRP laminate was better in loading efficiency and ductility of reinforced concrete short columns taking cost in consideration as well.

2. Experimental Program

To study the impact of utilizing CFPR and GFRP sheets as a completely or partially strengthening, five columns made of reinforced concrete were experimentally tested, with a concrete compressive strength of f_{cu} =34 N/mm^2

2.1 Samples for Testing

The cross section of each tested column was 200 by 200 mm, with a height of 1200 mm. The specimens were separated into two groups in addition to the control specimen: the first group consists of columns that were reinforced with CFPR sheets and second group includes columns at which strengthened by GFRP sheets. To verify the best method for increasing the loading capacity of reinforced concrete columns, fully and partly CFRP and GFRP sheets were selected. Table 1 Provides information about all specimens' reinforced concrete columns, Table 2 Provides details about each specimen's strengthening. While Figure 1 Displays the size of the specimen and the layout of the FRP jacket, Figure 2 demonstrates all column specimens after the formation of the FRP jacket**.**

2.2. Mixture of Concrete and Casting

Table 3 displays the concrete mix used for grade 34 MPa. Ordinary Portland cement, natural sand, and crushed natural dolomite material with a maximum nominal size of 10 mm were utilized to produce the concrete mixture. To preserve their form and shape, the test specimens were vertically cast in wooden forms that were braced with battens.

Table1 Information about all specimens reinforced concrete columns

Specimen	fcu (N/mm2)	Dimensions (mm)	Steel Reinforcement		
			Long. bars		Stirrups
			Type	fy (N/mm2)	
C00	34	200x200x1200	4T12 mm	500 N/mm2	6T8/m
C02					
C03					
C04					
C05					

Table 2 Details about each specimen's strengthening

Specimen	Strengthening configuration		
	Type	Wrapping	Size (mm)
C00	Control	N/A	N/A
C02	CFRP	Fully	1x900x1200
C03	CFRP	Partially	6x900x100
C04	GFRP	Fully	1x900x1200
C05	GFRP	Partially	6x900x100

Table 3 Concrete mixing proportions in kg /m^3

Cement	Water	Aggregate	Sand	w/c ratio
360	180	1200	600	0.5

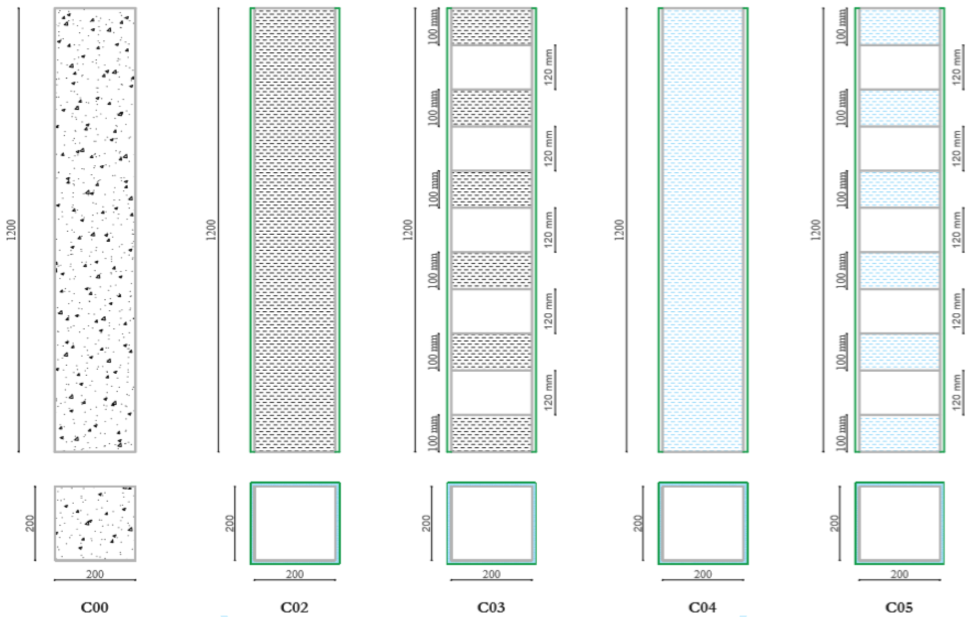

Fig. 1 Size of the specimen and the layout of the FRP jacket

Fig. 2 Specimens after the formation of FRP jacket

Concrete's characteristic compressive strength and splitting tensile strength were tested experimentally in order to evaluate hardened concrete. When three standard cubes and cylinders were evaluated after 28 days, the average values for compressive strength and splitting tensile strength were 34 MPa and 3.5 MPa, respectively.

2.3 Column Specimens Preparing

Wooden forms were prepared for all column specimens as presented in Figure 3(a), strain gauges with 120 ohms ± 0.2 were installed for selected longitudinal and transverse steel reinforcement as shown in Figure 3(b) and Figure 3(c).

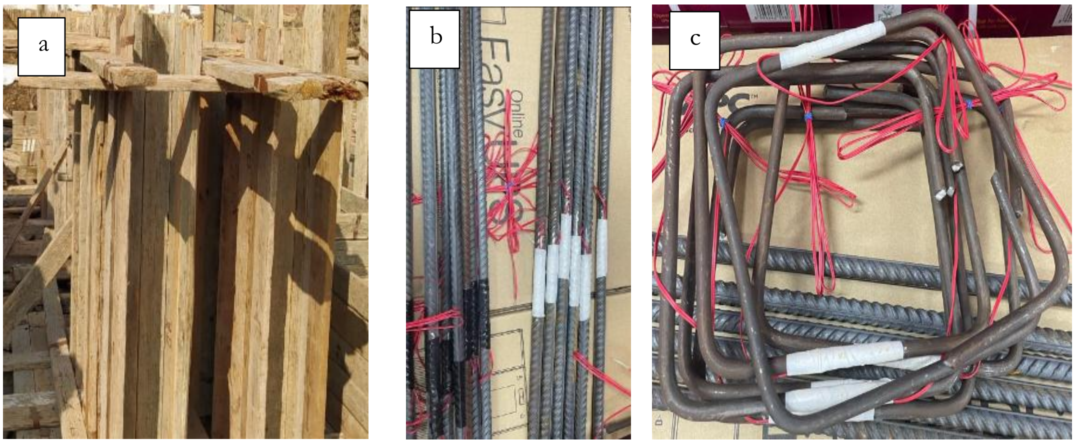

Fig. 3 (a) Wooden forms, (b) Strain gauges for longitudinal reinforcement, (c) Strain gauges for stirrups reinforcement

Figure 4 presented sequence and procedures for preparing column specimens corner curvature to ensure the confinement effectiveness of column areas. Also, be sure to tighten CFRP and GFRP laminates during installation, generating an adequate overlap of at least 10 cm. All of these steps are performed to ensure the success of CFRP and GFRP bonding throughout the experimental test, which improves the columns' ability to withstand more loads. Consequently, mixing resin components before placing on column specimens, placing resin bonding material on the column faces before wrapping processes and apply pressure using a roller to ensure that the resin was absorbed from column and CFRP laminates. The details CFRP and GFRP strengthening method for columns have been provided in an attempt to help structural engineers to understand the processes involved in applying this type of strengthening, particularly because it has demonstrated significant enhancement in practical tests.

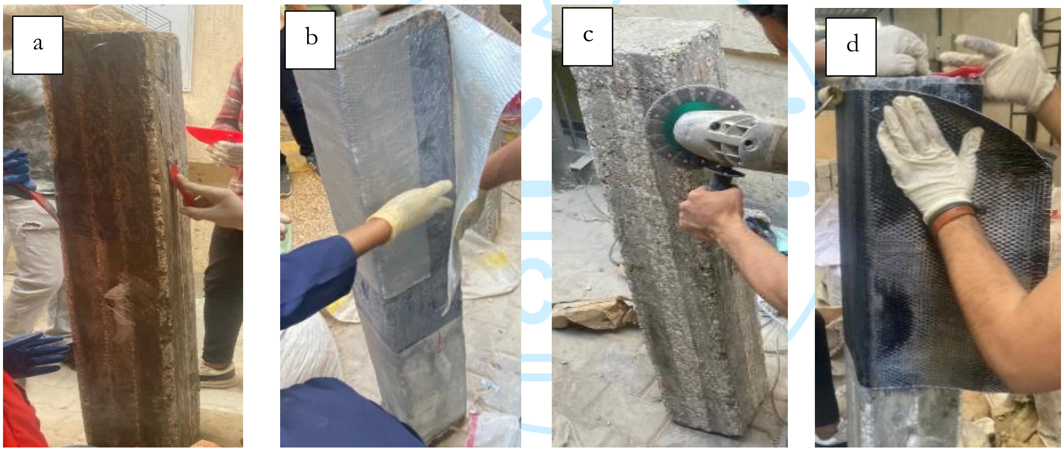

Fig. 4 Processing of corner curvatures and wrapping GFRP and CFRP laminates, (a) placing resin bonding material, (b) Fully wrapping GFRP laminates, (c) Making corner curvatures, (d) Fully wrapping CFRP laminates

2.4. Method of Testing

The specimens were positioned between the steel plates and the load cell in the loading frame equipment. The data logger system was linked to the computer along with the load cell, strain gauges, and linear voltage displacement transducer (LVDT). For the columns made of reinforced concrete, the steel plates offer consistent bearing surfaces. A 5000 kN. load cell recorded the load. Figure 5 illustrates a schematic depiction of the test setup.

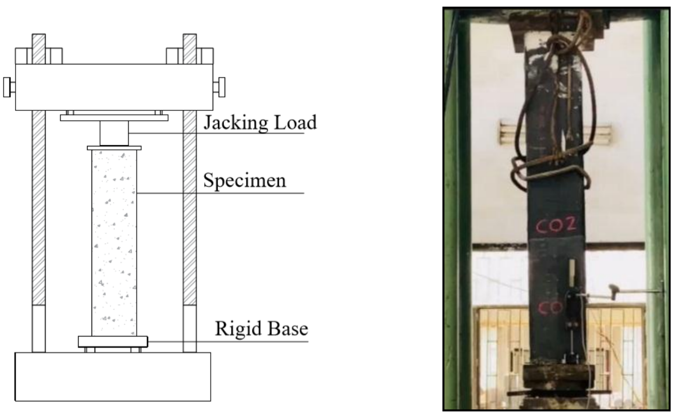

Fig. 5 Schematic depiction of the test setup

3. Test Results

3.1 Crack Pattern and Mode of Failure

The arrangement and design of the FRP jacket affected the crack pattern and mechanism of failure. Especially, in specimens with fully FRP jacket, neither the original crack nor the cracking load could be seen. On the other hand, samples with partially FRP jacket may monitored load of failure and ultimate corresponding shortening for all specimens presented in Table 4.Consequently, the relationship between applied load and corresponding shortening for all experimental specimens presented in Figure 6. For control specimen C00, near the top of the column head, slanted fractures began to show as the weight rose. the number and width of the cracks increased with the increasing of the load. Figure 7 illustrates how the concrete cover spalled off at around 92% of the column's failure load (820kN), causing a noticeable buckling of the longitudinal reinforcement and outer buckling in the transverse reinforcement (stirrups) on one side. The specimen completely collapsed and crushing damage was noticed when the force reached 891.2 kN. For sample C02 at which the column is fully wrapped by CFPR sheets, As the load increased, the cracks eliminated because of positive impact of CFRP wrapping, the load capacity of the specimen enhanced at which reached to 1250.5 kN with 9.05mm for axial shortening until sudden CFRP rupture occurred as presented in Figure 7.

Specimen C03 at which partially confined by CFRP laminates, some of cracks appeared in between wrapped CFRP as shown in Figure 7. Eventually, the cracks propagated aggressively at third upper zone of the column with load level of 96% from failure load of the column (994kN) with monitored corresponding shortening of 11.7 mm. Mode of failure for column specimen C04 was presented in Figure 7 at which GFRP laminates was ruptured smoothly and the load values remain semi constant. Also, the ability of column to sustain shortening and strain in reinforcement was increased without substantial losses in loads. For specimen C04 at which partially confined by GFRP laminates as presented in Figure 7, the cracks aggressively propagated at the lower third part of column. Sudden rupture failure for GFRP laminates occurred at load level of 975 kN and corresponding shortening with 8.6 mm.

Table 4 load of failure and ultimate corresponding shortening for all samples

Sample	load of failure Pu (kN.)	Pu/Pu (control)	Δu (Shortening) (mm)	Δu/Δ $_{Control}$
C00	891.20	1.00	8.42	1.00
C02	1250.50	1.40	9.05	1.07
C03	1035.50	1.16	12.46	1.47
C04	1060.00	1.19	11.41	1.35
C05	973.50	1.11	8.65	1.03

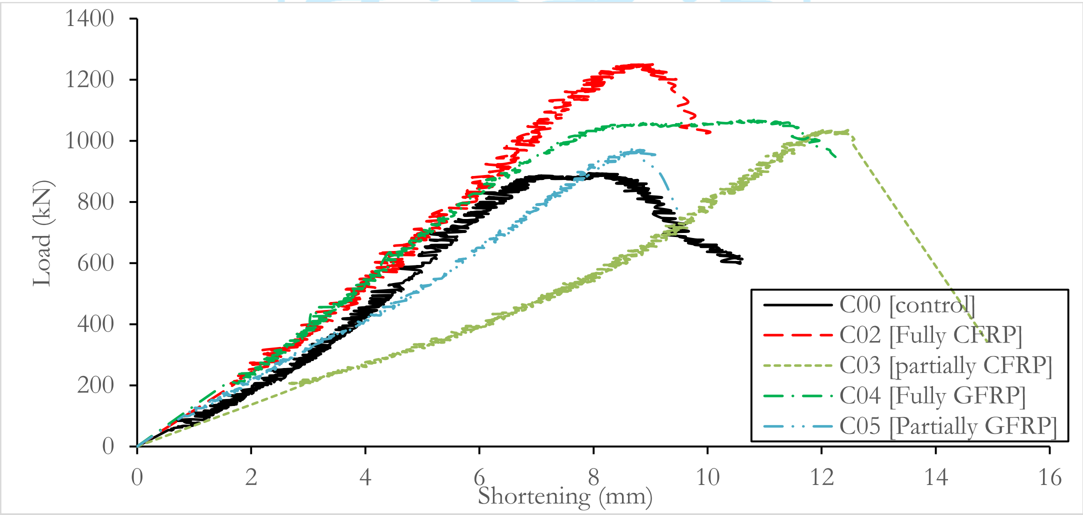

Fig. 6 Load-shortening relationship for all specimens.

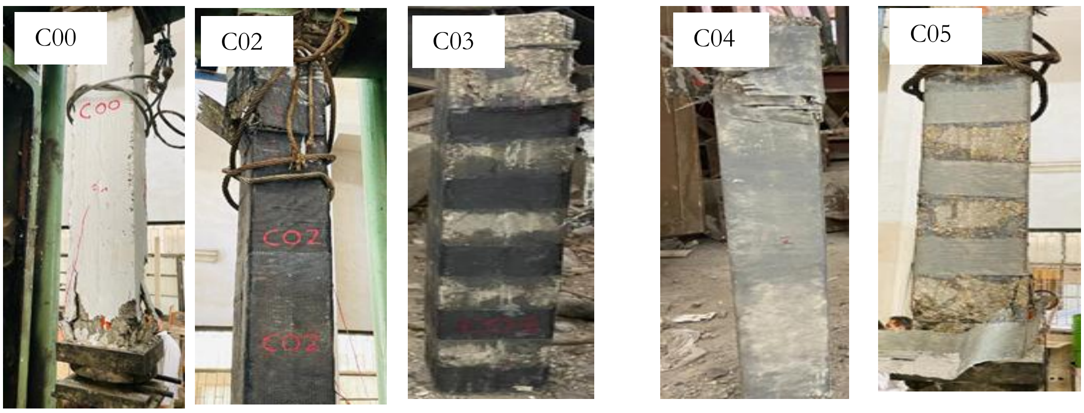

Fig. 7 Failure Mode for all examined specimens

3.2 Strains in Longitudinal and Transverse RFT

Each specimen had two strain gauges to monitor and record the strains in longitudinal and transverse steel reinforcements. The longitudinal strains and transverse steel reinforcement were recorded at the upper third for all column specimens. Figure 8a shows the load versus strains in longitudinal and transverse bars of control column sample C00. The longitudinal bar's strain was observed to have attained its maximum yielding point value of 0.0025 at a maximum load of 891.2 kN. Conversely, at the same peak load, the stirrups bar strain measurement was 0.0002. This confirms that the number of used stirrups was sufficient to accommodate the indirect tension resulting from direct compression. Figure 8b represent the relation between applied load and corresponding strains in longitudinal and stirrups bars at which equal 0.0014 and 0.0003 respectively for specimen C02. Decreasing in the value of longitudinal RFT strain and didn't reach the yielding point confirmed the effectiveness of confinement concrete by CFRP fully jacket. So, the ability to resist compression load increased by 40% with the negative effect of decreased ductility by 18% compared to control specimen. Figures 8c, 8d and 8e show the relation between load and corresponding strains for longitudinal and transverse reinforcement for specimens C03, C04 and C05 respectively. Consequently, these column specimens behave the same as the values of strain values for confined specimen C02. This behavior has also been explained previously.

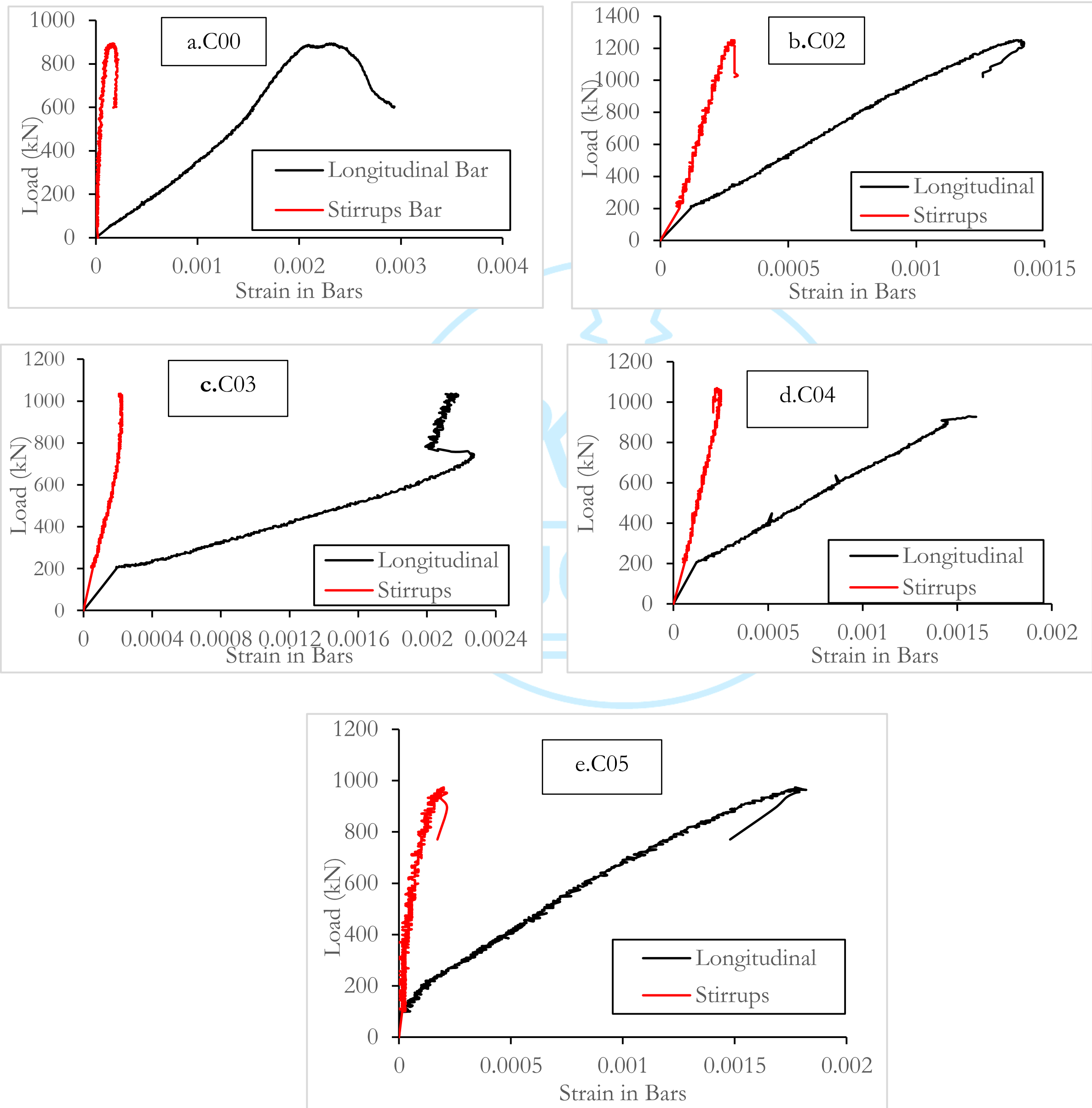

Fig. 8 Load versus strains in longitudinal and transverse bars for all specimens

3.3 Energy Absorption and Ductility

Ductility (D) can be described as the ability of column specimens to dissipate and absorb energy and deflection without failure occurred which could be expressed as the proportion between the greatest and minimum values of shortening at 80 % from failure load. Consequently, energy absorption is defined as the toughness of the column specimens at which could be calculated as the area under the curve of the load shortening relationship. Compared to control column specimen C00, the ductility index decreased for specimens C02 and C03 by 19% and 26% respectively. Consequently, the maximum load capacity enhanced by 40% and 16% respectively for the same two specimens. For specimen column C04 which fully wrapping by GFRP sheets, the load capacity slight increased by 19% compared to control column specimen and also, the ductility increased by 15%. Specimen C04 is the only experimental specimen that increased the column capacity to bear loads without decreasing the ductility. To a large extent, energy absorption was at the same trend of ductility. However, energy absorption has a relative different consideration because it depends on the stiffness of column specimens at which represented by the ability of confinement concrete to resist the external loads because GFRP and CFRP sheets. Table 5 presented ductility and energy absorption for all specimens.

Table 5 Maximum load, maximum shortening, ductility index, and energy absorption for each tested column

Sample code	Maximum Load (kN)	Maximum Shortening (mm)	Ductility Index (D)	D/D control	Energy Absorption
C00	891.20	8.42	1.83	1.00	5561.50
C02	1250.50	9.05	1.50	0.82	6602.46
C03	1035.50	12.46	1.34	0.74	7453.40
C04	1060.00	11.41	2.10	1.15	8713.51
C05	973.50	8.65	1.35	0.74	4813.68

4. Numerical Analysis

4.1 Simulated of Concrete Columns

For every experimental column specimen, non-linear finite element analysis (NLFEA) with ANSYS 19 had been performed.

4.2 Concrete and Steel RFT

The behavior of concrete was simulated using ANSYS's non-metal plasticity model Solid 65. This model takes into account two failure mechanisms: uniaxial cracking and crushing strength [18]. Concrete is thought to have linear-elastic tensile behavior up until the point of crack initiation, which is correlated with the uniaxial cracking strength. Concrete's negative stiffness was defined by the crushed stiffness factor. For uniaxial compression behavior of high strength concrete, a linear connection between stress and strain is taken into consideration up to 30% of peak strength (fc'). On the other hand, steel RFT was simulated using Link180 axial loaded model.

4.3 Features of Laminates Made Of GFRP and CFRP

All mechanical characteristic of used CFRP and GFRP laminates get from technical data sheets of manufacturer product data sheets which presented in Table 6.

Table 6 Manufactures reported FRP system properties

Type	Ultimate Tensile strength f^*_{fu} (MPa)	Modulus of Elasticity E_f (GPa)	Rupture strain ε^*_{fu}	Thickness per ply t_f (mm)
CFRP	3500	225	0.018mm/mm	0.129
GFRP	1500	70	0.027mm/mm	0.129

5.3 D Finite Element Column Models

5.3.1 Control Column Specimen C00

In this section, 3D FE models were presented using ANSYS19 software. Figure 9(a) shows meshing for control concrete column C00 and the modeled bearing upper and lower plates. The longitudinal and transverse reinforcement, supported plates were presented in Figure 9(b). The upper plate was loaded by multiple points of loads to simulate the experimental load cell, consequently, the lower bearing plate were constrained at y directions for all points. It could be noted that the lower bearing plate also constrained in two points for x and z directions staggered with each other. This is to prevent the column from twisting during load application so, the vertical compression applied load becomes pure without any eccentricity as same in the experimental program. Figure 9(c) shows the pattern of crack and failure mode at which cracks propagation confirmed that the behavior is similar to the cracks development in the practical results. This convergence in results between numerical analysis by ANSYS and experimental gives confidence in the finite element simulation. The load versus shortening for experimental and NLFEA presented in Figure 9(d) for specimen C03. The comparison showed that there is a satisfied convergence between NLFEA and experimental results.

5.3.2 Column Specimen C02

In this specimen, the column was fully reinforced by CFRP laminates at which all nodes between CFRP laminates and concrete columns were coupled at x, y and z translations and rotations. This hypothesis was based on the fact that CFRP sheets were cohesively bonded throughout the practical loading test and these CFRP sheets didn't desponded. Figure 10(a) shows the modelling of coupling in NLFEA, Mode of failure for CFRP jacket and crack pattern of concrete behind CFRP jacket was presented in Figure 10(b). the crack pattern and failure mechanism confirmed that the behavior is very close to the crack's development in the experimental test. Figure 10(c) show the relation between load and corresponding shortening in column C02 at which showed differences up to 5% between experimental and NLFEA results.

5.3.3 Column Specimen C03

Specimen C03 deal with partially CFRP confining for concrete column as presented in Figure 11(a). The coupling model between CFRP sheets and concrete columns was created. Figure 11(b) show crack pattern in between and behind CFRP laminates where the results were very close to the experimental investigations. Figure 11(c) show the relation between load and corresponding shortening in column C03 at which showed differences up to 5% between experimental and NLFEA results.

5.3.4 Columns C04 and column C05

Columns C04 and column C05 were strengthened fully and partially GFRP sheets respectively as same but using GFRP sheets instead of CFRP sheets. The results could be followed in Table 7 in which in this table, comparison between ultimate load, shortening for experimental and FEA results were presented. Consequently, observed failure mode was mentioned for all column samples.

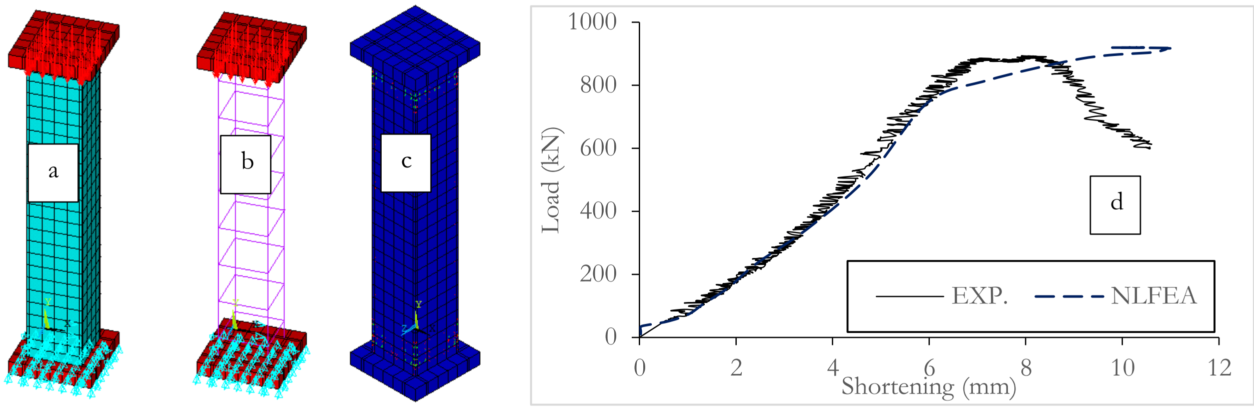

Fig. 9 NLFEA model and results for control column C00, (a) FE meshing, (b) Steel RFT, (c) Crack pattern, (d) Experimental and NLFEA results

1st principal stresses for partially confined CFRP were presented in Figure 12(a) at which principal stresses could be an indicator to determine if the CFRP material is failed or not. On the other hand, von misses stress presented in Figure 12(b) which is suitable for computing the safety factor against failure. The results showed that 1st principal stresses divided by von misses' stresses approximately equal 4%. Displacement vector sum for partially CFRP laminates also presented in Figure 12(c).

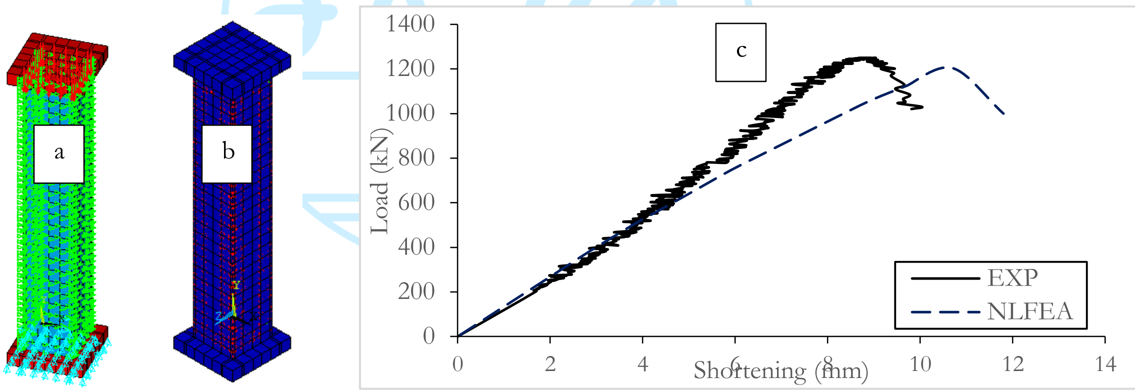

Fig. 10 NLFEA model for column C02 [Fully CFRP], (a) Coupling modelling, (b) Crack pattern, (c) Experimental and NLFEA results

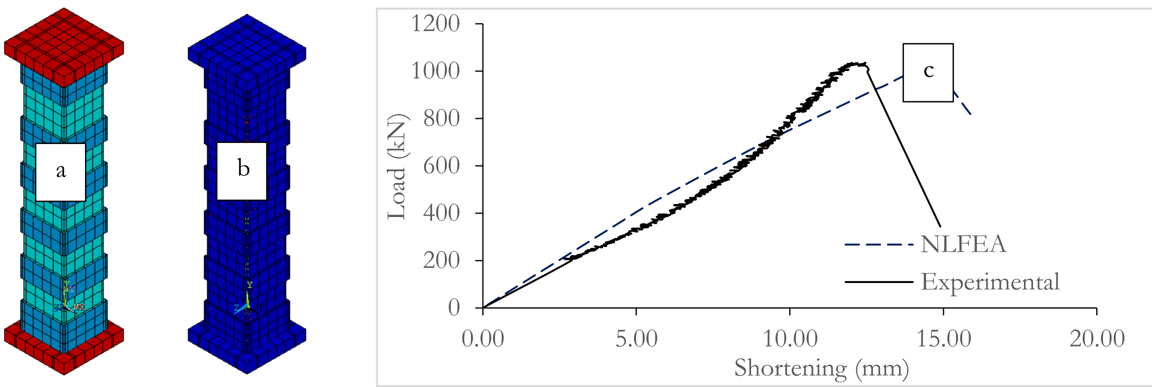

Fig. 11 NLFEA model for column C03 [Partially CFRP], (a) Partially confining, (b) Crack pattern, (c) Experimental and NLFEA results

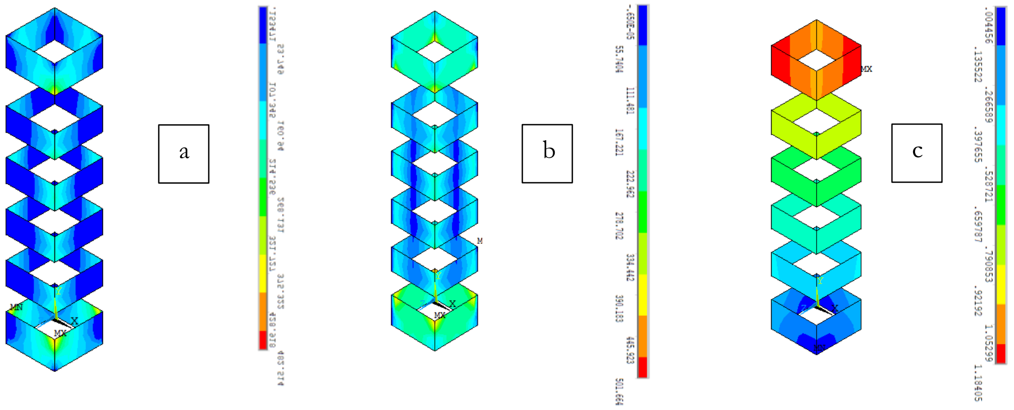

Fig. 12 Major straining actions for partially CFRP laminate, (a) 1st principal stresses, (b) Von misses' tensile strength, (c) Displacement vector sum

Table 7 Comparison between ultimate load, shortening and failure mode for experimental and FE results of all examined columns.

Samples Code	Ultimate load, Pu (kN)		$P_{u\ (Exp.)}$/ $P_{u\ (FEA)}$	Shortening, Δ_u (mm)		Failure Mode
	Results from experimental	Results of FE model		Results from experimental	Results of FE model	
C00	891.20	918.00	0.97	8.42	11.05	Concrete crushing
C02	1250.50	1204.00	1.04	9.05	10.70	FRP- Rupture
C03	1035.50	1000.00	1.03	12.46	14.60	Concrete crushing with FRP- Rupture
C04	1060.00	1020.00	1.04	11.41	13.20	FRP- Rupture
C05	973.50	964.40	1.01	8.65	9.43	Concrete crushing with FRP- Rupture

6. **Theoretical Predictions**

These theoretical expectations technique will aid in the development of conclusions regarding the suitability of various confinement CFRP and GFRP laminate configurations that are taken into consideration in this work.

6.1 ACI 440.2R-08 [19]

Strength and ductility of reinforced concrete columns can be increased by confining them with fiber-reinforced polymer (FRP) jackets [20].

For non-circular column cross sections and wrapping with FRP jacket which provide strength enhancement through the following equations:

$$\Phi P_n = 0.8\Phi\left[0.85 f'_{cc}\left(A_g - A_{st}\right) + f_y A_{st}\right] \qquad (1)$$

Where:

Pn: Predicted ultimate loading capacity of column
Ag: gross area of column, Ast: longitudinal steel reinforcement area
fcc': Concrete's confined characteristic strength
fy: yield strength of the longitudinal steel reinforcement

$$f'_{cc} = \psi_f x 3.3 x k_a x f_l \qquad (2)$$

$$f_l = \frac{2E_f n t_f \varepsilon_{fe}}{D} \qquad (3)$$

$$D = \sqrt{b^2 + h^2} \qquad (4)$$

$$K_a = \frac{A_e}{A_c}\left(\frac{b}{h}\right)^2 \qquad (5)$$

$$\varepsilon_{fe} = k_\varepsilon \varepsilon_{fu} \qquad \text{Assume } k_\varepsilon = 0.58 \qquad (6)$$
8

$$\frac{A_e}{A_c} = \frac{1 - \frac{\left[\left(\frac{b}{h}\right)(h-2r_c)^2 + \left(\frac{h}{b}\right)(b-2r_c)^2\right]}{3A_g} - \rho_g}{1-\rho_g} \qquad (7)$$

The FRP-confined concrete's maximum compressive strain ε_{ccu} could be determined as following:

$$\varepsilon_{ccu} = \left(\varepsilon'_c 1.50 + 12k_b \frac{f_l}{f'_c}\left(\frac{\varepsilon_{fe}}{\varepsilon'_c}\right)^{0.45}\right) \quad (8)$$

$\varepsilon_{ccu} \leq 0.01$

Where:

f_l: Confining strength due to FRP wrapping
D: Equivalent circular cross section diameter
Ka: Confined coefficient factor
ρ_g: Percentage of longitudinal steel reinforcement

6.2 ECP 208-2005[21]

The ultimate column capacity subjected to axial compression loads strengthened by fully or partially CFRP or GFRP laminates could be estimated according to the following equations:

$$P_u = 0.35 f_{cuc} A_c + 0.67 f_y A_{sc} \quad (9)$$

Where:

P_u : Ultimate load capacity of column
f_{cuc}: Apparent compressive strength due to wrapping
A_c : Area net of concrete
f_y : Yield strength of steel reinforcement
A_{sc} : Area of Longitudinal steel reinforcement

$$f_{cuc} = f_{cu}\left[2.25\sqrt{1 + 9.875\frac{f_l}{f_{cu}}} - 2.5\frac{f_l}{f_{cu}} - 1.25\right] \quad (10)$$

Where:

f_{cu}: Characteristic compressive strength
f_l : Lateral confinement strength of column

$$f_l = K_e \frac{\mu_f E_f \varepsilon_{fe}}{2\gamma_f} \quad (11)$$

$$\mu_f = \frac{2nt_f(b+t)}{bt} \quad (12)$$

μ_f: Volume percentage of FRP wrapping for rectangle columns

$$K_e = 1 - \frac{(b-2r_c)^2 + (t-2r_c)^2}{3(bxt)(1-\mu_s)} \quad (13)$$

Where:

K_e: Confined effectiveness coefficient
μ_s: Percentage of longitudinal steel reinforcement in column
r_c: Curvature radius at column corners

For partially confined concrete column, there is additional confined effectiveness coefficient along the column height multiplied in lateral condiment strength of column.

$$K_{e2} = \frac{(b-\frac{s_c}{2})(t-\frac{s_c}{2})}{b.t} \quad (14)$$

Table 8 Comparison between ultimate load for experimental, FE results and theoretical Expectations of all examined columns.

Samples Code	Ultimate load, Pu (kN)			
	Results from experimental	Results from FE model	Theoretical Expectations	
			ACI 440.2R-08	ECP 208-2005
C00	891.20	918.00	738.86	627.42
C02	1250.50	1204.00	964.50	820.90
C03	1035.50	1000.00	818.04	724.80
C04	1060.00	1020.00	946.20	731.40
C05	973.50	964.40	771.25	8691.18

7. Conclusions

Based on experimental, finite element and theoretical results for strengthening concrete columns using fully or partially wrapped CFRP and GFRP laminates, conclusion could be presented as following:

- Strength and energy absorption of reinforced concrete columns can be increased by confining them with GFRP or CFRP jackets.
- Fully CFRP wrapping for concrete columns had a great enhancement of confinement concrete at which loading capacity level improved by 40% compared to control column specimen.
- All examined strengthened concrete columns lost ductility by different ratios, except specimen C04 which fully wrapped by GFRP laminates, ductility enhanced by 15% compared to control column specimen C00.
- Sample C05 at which partially wrapped by GFRP had a slight enhancement in loading capacity level reached 9.2% with ductility decreasing by 26%.
- CFRP and GFRP jackets were more effective in the upper and lower thirds zones for strengthened short columns. This conclusion could be confirmed by pattern of crack and failure mode for all examined samples.
- Numerical analysis results were fairly satisfactory when compared to experimental results with an average of 5% however, it exhibited principal stresses and strains within CFRP or GFRP wrapping which provided a more comprehensive understanding for its behavior.
- Theoretical expectations whether using ACI 440.2R-08 or ECP 208-2005 was conservative in calculating loading capacity of columns in which strengthened by fully or partially CFRP or GFRP laminates.
- Ultimate load capacity prediction for control column specimen without any strengthening using ECP 208-2005 was more restrained than ACI 440.2R-08 in which all obtained code values were less than experimental results by 17 % and 30 % for ACI 440.2R-08 and ECP 208-2005 respectively.
- Prediction for strengthened column specimens by FRP system using ECP 208-2005 was more restrained than ACI 440.2R-08 in which all obtained code values were less than experimental results by 23 % and 35 % for ACI 440.2R-08 and ECP 208-2005 respectively.
- As an extension investigation for this research, it could be modelled the shear stiffness of resin material interface between concrete columns and composite materials.

Acknowledgments

The authors wish to acknowledge the support of the concrete Lab in Faculty of Engineering, Zagazig University, Zagazig, Egypt

Conflict of Interest

The authors have no financial interest to declare in relation to the content of this article.

References

1. Haytham F Isleema, Muhammad Tahirb and Zhenyu Wang 2020 Axial stress–strain model developed for rectangular RC columns confined with FRP wraps and anchors Structures 23 779-788
2. Damian K, Thomas M, Solomon Y, Kasidit C, Tanarat P. Finite Element Modeling of Reinforced Concrete Structures Strengthened with FRP Laminates. Report published under supervision of, Oregon Department of Transportation (ODOT) Research Group and Federal Highway Administration; 2001.
3. N. Pasala, S. Dipti, R. Durgesh, Seismic strengthening of RC columns using external steel cage, Earthquake Eng. Struct. Dyn. J. 38 (2009) 1563-1586.
4. Khair B. Retrofitting of Square Reinforced Concrete Columns Subjected to Concentric Axial Loading with Steel Jackets, in: The Third Engineering Consultant work conference, Palestine, 2009.
5. Shamim A Sheikha and Yimin Li 2007, Deisgn of FRP confinement for square concrete columns. Engineering Structures 29, 1074-83.
6. Mini K Madhavan, Dhanya Sathyan and Karingamanna Jayanarayanan 2021 Hybrid natural fiber composites in civil engineering applications, Hybrid natural fiber composites chapter 3.
7. Cheng Chen, Yancai Yang, Yingwu Zhou, Chunrun Xue, Xu Chen, Haocong Wu, Lili Sui and Xue Li 2020 Comparative analysis of natural fiber reinforced polymer and carbon fiber reinforced polymer in strengthening of reinforced concrete beams Journal of cleaner production 263, 121572
8. M. Rosario, P. Vincenzo, reinforced concrete columns strengthened with angles and battens subjected to eccentric load, Eng. Struct. 31 (2008) 539-550.
9. Cao, Y. G., Jiang, C. and Wu, Y. F. (2016). "Cross-Sectional Unification on the Stress-Strain Model of Concrete Subjected to High Passive Confinement by Fiber-Reinforced Polymer." Polymers 8, Vol.186.
10. Lam, L. and Teng, J.G. (2002). "Strength Models for Fiber-Reinforced Plastic- Confined Concrete." Journal of Structural Engineering, 128, 612–623.
11. Teng, J.G. and Lam, L. (2002). "Compressive Behavior of Carbon Fiber Reinforced Polymer-Confined Concrete in Elliptical Columns." Journal of Structural Engineering, 128, 1535–1543.

12. Lam, L. and Teng, J.G. (2003). "Design-Oriented Stress-Strain Model for FRP- Confined Concrete." Journal of Construction and Building Materials, 17, 471–489.
13. Lam, L. and Teng, J.G. (2003). "Design-Oriented Stress-Strain Model for FRP- Confined Concrete in Rectangular Columns." Journal of Reinforced Plastics and Composites, 22, 1149–1186.
14. Youssef, M.N., Feng, M.Q. and Mosallam, A.S. (2007). "Stress–Strain Model for Concrete Confined by FRP Composites." Journal of Composites, 38, 614–628.
15. Hu, B. and Wang, J.G. (2010). "Unified Model for Calculating Stress-Strain Relationship of Circular and Rectangular Concrete Columns Confined with FRP." J. Xi'an University of Architecture and Technology, 4, 394–406.
16. Wei, Y.Y. and Wu, Y.F. (2012). "Unified Stress-Strain Model of Concrete for FRP- Confined Columns." Journal of Construction and Building Materials, 26, 381–392.
17. Chastre, C. and Silva, M.A.G. (2010). "Monotonic Axial behavior and modeling of RC circular columns confined with CFRP." Engineering Structures, vol. 32, 2268-2277.
18. Mohamed M. Badawy, Azza I. Anan, Omar A. Elkadi, Ezzeldin Y. Sayed-Ahmed. "Flexural behavior of high strength concrete shallow wide beams reinforced by hybrid longitudinal reinforcement", HBRC Journal, 2024
ACI 440.2R-08 "Guide for the Design and Construction of Externally Bonded FRP Systems for Strengthening Concrete Structures" ACI Committee 440, American Concrete Institute, Farmington Hills, MI, 2005, pp.16.
19. Teng, J.G. and Lam, L. (2004). Behavior and Modeling of Fiber Reinforced Polymer-Confined Concrete. Journal of Structural Engineering, 130(11), pp.1713–1723.doi: https://doi.org/10.1061/(asce)0733-9445(2004)130:11(1713)
20. Egyptian Ministry of Housing, Utilities, & Urban Development (2005), 'Egyptian Code of Practice for the Use of Fiber Reinforced Polymer FRP) in the Construction Fields', Egyptian Housing and Building National Research Center, Code no. ECP 208-2005, 160 pp.